SUPPLEMENTARYMATERIALS.

Effects of ACE mutations associated with Alzheimer's disease on blood ACE phenotype

Olga V. Kryukova[1], Igor O. Islanov[2], Elena V. Zaklyazminskaya[2], Dmitry O. Korostin[3], Vera A. Belova[3], Valery V. Cheranev[3], Zhanna A. Repinskaia[3], Maxim Y. Shkurnikov[4], Aleksander G. Tonevitsky[4], Pavel A. Petukhov[5], Steven M. Dudek[6], Olga A. Kost[1], Denis V. Rebrikov[3] and Sergei M. Danilov[6].

[1]Faculty of Chemistry, M.V. Lomonosov Moscow University, Moscow, Russia, so.b11onde@gmail.com, olga.a.kost@gmail.com
[2]MedicalGenetics, Petrovsky National Research Centre of Surgery, Moscow, Russia,
[3]Center for Precision Genome Editing and Genetic Technologies for Biomedicine, Pirogov Russian National Research Medical University, Moscow, Russia,
[4]Faculty of Biology and Biotechnology, National Research University Higher School of Economics, Moscow, Russia,
[5]Department of Pharmaceutical Sciences, College of Pharmacy, University of Illinois, Chicago, IL, USA,
[6]Department of Medicine, Division of Pulmonary, Critical Care, Sleep and Allergy, University of Illinois at Chicago, IL, USA.

Running Head: ACE mutations and blood ACE levels

*Corresponding author:
Sergei M. Danilov, MD, PhD
Department of Medicine,
Division of Pulmonary, Critical Care, Sleep and Allergy,
University of Illinois at Chicago
CSB 915, MC 719, 840 S. Wood Ave.
Chicago, IL60612
Phone: (708)-642-0635,
E-mail:danilov@uic.edu

Key words: Angiotensin I-converting enzyme, mutations, conformational changes, blood ACE, screening, Alzheimer's disease

Fig.S1. Effects of ACE mutations on mAbs binding to mutant ACEs.

A. ACE was precipitated from the EDTA-plasma of subjects with different mutations using mAbs 9B9 and i1A8 to the N domain of ACE. ACE activity was quantified fluorometrically using HHL as a substrate as described in Fig.2. Data are presented as the 9B9/1IA8 binding ratio expressed as % obtained from control patients without ACE mutations.

B-F. Precipitated ACE activity was determined in the plasma of carriers of different ACE mutations as in **A,** but using mAbs 1G12 and 5F1, and expressed as (**B, C**) precipitated ACE activity (% of control samples without ACE mutations) and (**D**) as the 1G12/5F1 binding ratio for each mutant (% of control). Each value represents the mean of 3-5 independent experiments. Coloring is the same as in Fig.2.

Figure S2. Localization of theY215C mutation in the N domain of ACE.

Shown is the Cryo-EM structure of truncated (1-1201) human somatic ACE (PDB 7Q3Y) [29] using molecular surface representation. Key amino acids are denoted using somatic ACE numbering. The surface is colored light beige. Specific amino acid residues are colored as following: Asn as putative glycosylation sites are highlighted in green; ACE Y215C mutation is highlighted in magenta; the last visible residue in the C-terminal end of this truncated somatic ACE is marked by its amino acid number (1201). The epitopes for the mAbs to the N domain (9B9, 1G12, 5F1) and the C domain (2H9) that are used to analyze these blood samples are marked by 30 Å diameter black circles, which correspond to an approximately 700 $Å^2$ area covered by each mAb.

Fig. S3. Conformational mAb fingerprinting of ACE mutations (P476A and G610S).

ACE activity in subjects with P476A and G610S ACE mutations was determined from EDTA-plasma samples after precipitation by 7 different mAbs to the N and C domains of ACE as described in Fig.2.

A-B. ACE activity determined with ZPHL as a substrate expressed as a % of control samples.

C-D. Data represent the ZPHL/HHL binding ratios expressed as % of controls.

E. Shown is the Cryo-EM structure for the residues 450-613 of human somatic ACE (PDB 7Q3Y) [29] displayed as a ribbon presentation. ACE mutations P456R, P476A, P601L and G610S are highlighted with magenta. Putative glycosylation sites (N480 and N494) are highlighted with green. The 472-498 C2-loop (as defined in [29]) is highlighted with grey. Highlighted in red are the residues K489 and Y498 within the cleft of the active center. A Zn^{2+} ion is also shown.

Previously we established the **ACE phenotyping** approach for comprehensive characterization of ACE in the blood. This approach includes not only measurement of blood ACE activity with different substrates and estimation of catalytical properties, but also quantification of immunoreactive ACE protein and conformational changes in ACE molecules using a wide set of mAbs [22,23,25,26,31,32].

Unfortunately, most sequencing facilities have access to only EDTA-plasma samples, which prevent direct measurement of ACE activity and estimation of catalytic properties of mutant ACEs. Nevertheless, using mAbs to ACE which we have generated in combination with multiple ACE substrates allows for the precipitation of ACE from EDTA-plasma samples and estimation of ACE activity. With this approach we can characterize the effects of ACE mutations in fine detail from EDTA-plasma samples.

When we performed primary estimation of the blood ACE levels in EDTA-plasma samples for different ACE mutations (Fig.2,5), we used strong, high-affinity mAbs 9B9 and 1G12 [24] for precipitation of the enzyme. Precipitated ACE activity quantified by these mAbs generally did not depend on the nature of substrates which we used (ZPHL or HHL) (not shown). However, when we perform conformational fingerprinting of mutant ACE using a wider set of mAbs, we need to consider that precipitation of ACE activity with some weak mAbs may be substrate-specific. This is possible because immobilization of some mAbs on plates can result in anti-catalytic properties

toward the N or C domain active center when precipitating ACE (see below in Fig.S4). Therefore, the preferred approach should be to use HHL for the quantification of precipitated ACE activity with mAbs to the N domain (because HHL is cleaved 9-fold more effective by the C domain active center), while ZPHL should be used for precipitation of ACE activity with mAbs to the C domain active center - discussed in [27].

As an example, the effect of ACE mutation Y215C on the 9B9/i1A8 ratio (Fig.S2A) was decreased only with HHL as a substrate, while the effect of this mutation on this ratio was absent with ZPHL as a substrate (not shown).

One of the goals of this study was to test multiple mAbs and substrates to determine a combination which will allow for the detection of mutant ACE in the blood and distinguish it from native (control) ACE. Identification of markers for ACE mutations will provide a method for monitoring changes in mutant ACE activity in the blood. Such an approach would be particularly useful for assessing the effectiveness of therapies designed to increase surface ACE expression. We hypothesize that this type of therapeutic strategy could be protective for some patients at risk for ACE-dependent Alzheimer's disease. Fig.S1B-D describes the effects of different ACE mutations on the precipitation of blood ACE activity by mAbs 1G12 and 5F1. The binding of mAb 5F1 was **increased** in ACE mutant G325R and **decreased** in ACE mutant P476A. Therefore, the 1G12/5F1 binding ratio could be a convenient marker for these two ACE mutations, G325R and P476A. These results could be especially important for carriers of the G325R ACE mutation because it is likely damaging and results in a transport-deficient ACE (Fig.2,5). Carriers of this mutation may benefit from rescue of impaired trafficking of mutant ACE to the cell surface through use of a cocktail of chaperones and protease inhibitors as we have previously described for the Q1069R ACE mutation [14].

Our results provide additional insights into the functional consequences of these mutations. The effects of the P476A mutation on ACE activity after precipitation by different mAbs (Fig.S3A)

and the localization of this mutation in the ACE protein (Fig.4 and Fig.3E) combine to shed light on the putative mechanism of action by which this mutation results in increased ACE shedding and altered catalytic properties (Fig.S3C and S3E).

Fig. S4. Effects of mAbs and various ACE mutations on the ZPHL/HHL ratio.

A. ACE was precipitated from EDTA-plasma samples of control subjects (without ACE mutations) using7 different mAbs to the N and C domains of ACE. ACE activity was quantified fluorometrically with ZPHL and HHL as substrates as described in Fig.2. ZPHL/HHL ratios are presented as % of that for mAb 9B9.

B-F. ACE activity was determined in plasma samples from carriers of different ACE mutations as in **A**. Data are expressed as ZPHL/HHL ratios for each mutant and mAb as % of control ACE activity (without ACE mutations). **B.** ACE activity results are presented individually from the plasma of patient #5534 with the Y215C mutation. Other values are presented as the mean from multiple carriers of a given mutation. **C**. G325R; **D**. P476A; **E**. G610S; **F**. R1250Q. Each value is a mean of 3-10 independent experiments. Coloring is the same as in Fig.2.

Quantification of the ZPHL/HHL ratio for carriers of these ACE mutations not only provided an explanation for catalytic changes in P476A (Fig.S3C, E), but this approach also helped to identify a marker for further study of an outlier in the Y215C group of ACE mutations (patient 5534 in Fig.2,5).

Table S1. Existing human ACE mutations.1234_62 (09/29/23)-
separate excel file due to high volume.

Table S2. 62 ACE mutations for which blood ACE levels were estimated or measured.
Separate excel file.

References for Table S1 and S2: ACE Mutations.1234_62.09.29.23

1. Uematsu M, Sakamoto O, Ohura T, et al, A further case of renal tubular dysgenesis surviving the neonatal period. *Eur J Pediatr* 2009; **168**: 207–209.
2. Gribouval O, Morinière V, Pawtowski A, et al. Spectrum of mutations in the renin-angiotensin system genes in autosomal recessive renal tubular dysgenesis. *Hum Mut*. 2012; **33**: 316–326.
3. Schreiber R, Gubler M-C, Gribouval O, et al. Inherited renal tubular dysgenesis may not be universally fatal. *Pediatr Nephrol* 2010; **25**: 2531–2534.
4. Kryukova OV, Islanov IO, Zaklyazminskaya EV, et al. Effect of ACE mutations, associated with Alzheimer's disease, on blood ACE phenotype. *Translat. Res.* (2024); (this study)
5. Xie X-Y, Zhao Q-H, Huang Q, et al, Genetic profiles of familial late-onset Alzheimer's disease in China: The Shanghai FLOAD Study. *Genes Dis* 2022; **9**: 1639–1649.
6. Gribouval O, Gonzales M, Neuhaus T, et al. Mutations in genes in the renin-angiotensin system are associated with autosomal recessive renal tubular dysgenesis. *Nat Genet* 2005; **37**: 964–968.
7. Sassi C, Ridge PG, Nalls MA, et al. Influence of coding variability in APP-Aβ metabolism genes in sporadic Alzheimer's disease. *PLOS One* 2016; **11:** e0150079.
8. Richer J, Daoud H, Geier P, et al. Resolution of refractory hypotension and anuria in a premature newborn with loss-of-function of ACE. *Am J Med Genet* 2015; **167A**: 1654-1658.
9. Kim SY, Kang HG, Kim EK, et al. Survival over 2 years of autosomal-recessive renal tubular dysgenesis. *Clin Kidney J* 2012; **5**: 56–58.
10. Michaud A, Acharya KR, Masuyer G, et al. Absence of cell surface expression of human ACE leads to perinatal death. *Hum Mol Genet* 2013; **23**: 1479–1491.
11. Tan H-J, Jian W-Y, Lv C, et al. Prenatal diagnosis and treatment for fetal angiotensin converting enzyme deficiency. *Prenat Diag* 2023; 1-5.
12. Kondoh T, Kawai Y, Matsumoto Y, et al. Management of a preterm infant with renal tubular dysgenesis: A case report and review of the literature. *Tohoku J Exp Med.* 2020; **252**: 9–14.

13. Persu A, Lambert M, Deinum J, et al. A Novel Splice-Site Mutation in Angiotensin I-Converting Enzyme (ACE) Gene, c.3691+1G>A (IVS25+1G>A), Causes a Dramatic Increase in Circulating ACE through Deletion of the Transmembrane Anchor. *PLoS One* 2013; **8**: e59537.
14. Nesterovitch AB, Hogarth KD, Adarichev VA, et al. Angiotensin I-converting enzyme mutation (Trp1197Stop) causes a dramatic increase in blood ACE. *PLoS One* 2009; **4**: e8282.
15. Danilov SM, Jain MS, Petukhov PA, et al. Novel ACE mutations mimicking sarcoidosis by increasing blood ACE Levels. *Transl Res* 2021; **230**: 5–20.
16. Danilov SM, Adzhubei IA, Kozuch AJ, et al. Carriers of heterozygous loss-of-function ACE mutations are at risk for Alzheimer's disease. *Biomedicines* 2024; **12**: 162.
17. Lalli M.A. et al. Exploratory data from complete genomes of familial Alzheimer's disease age-at-onset outliers. *Hum Mutat* 2012; **33**: 1630-1634.
18. Schwartzentruber J, Cooper S, Liu JZ, et al. Genome-wide meta-analysis, fine-mapping and integrative prioritization implicate new Alzheimer's disease risk genes. *Nat Genet* 2021; **53**: 392–402.
19. Samokhodskaya LM, Jain MS, Kurilova OV, et al. Phenotyping angiotensin-converting enzyme in blood: A necessary approach for precision medicine. *J Appl Lab Med* 2021; **6**: 1179–1191.
20. Rieder M, Taylor SL. Clark AG, Nickerson DA. Sequence variation in the human angiotensin-converting enzyme. *Nat Genet* 1999; **22**: 59-62.
21. Danilov SM, Wade MS, Schwager SL, et al. A novel angiotensin I-converting enzyme mutation (S333W) impairs N-domain enzymatic cleavage of the anti-fibrotic peptide, Ac-SDKP. *PLoS One* 2014; **9**: e88001.
22. Vincent KM, Alrajhi A, Lazier J, et al. Expanding the clinical spectrum of autosomal-recessive renal tubular dysgenesis: Two siblings with neonatal survival and review of the literature. *Mol Genet Genomic Med* 2022; **10**: e1920.

23. Danilov SM, Gordon K, Nesterovitch AB, et al. An angiotensin I-converting enzyme mutation (Y465D) causes a dramatic increase in blood ACE via Accelerated ACE shedding *PLoS One* 2011; **6:** e25952.

24. Ruf K, Wirbelauer J, Beissert A and Frieauff E. (2018) Successful treatment of severe arterial hypotension and anuria in a preterm infant with renal tubular dysgenesis—A case report. *Matern Health Neonat Perinat* 2018; **4**: 27.

25. Danilov SM, Lünsdorf H, Akinbi HT, et al. Lysozyme and bilirubin bind to ACE and regulate its conformation and shedding. *Sci Rep* 2016; **6:** 34913.

26. Nicolaou N, Pulit SL, Nijman IJ, et al. Prioritization and burden analysis of rare variants in 208 candidate genes suggest they do not play a major role in CAKUT. *Kidney Int* 2016; **89**: 476–486.

27. Ramoni RB, Himes BE, Sale MM, Furie KL, Ramoni MF. Predictive genomics of cardioembolic stroke. *Stroke* 2009; **40**: (*3 Suppl*), S67-S70.

28. Cuddy LK, Prokopenko D, Cunningham EP, et al. Aβ-accelerated neurodegeneration caused by Alzheimer's-associated ace variant R1279Q is rescued by angiotensin system inhibition in mice. *Sci Transl Med* 2020; **12**: eaaz2541.

29. Pescatello LS, Schifano ED, Ash GI, et al. Deep-targeted exon sequencing reveals renal polymorphisms associate with postexercise hypotension among African Americans. *Physiol Rep* 2016; **4**: e12992.

30. Danilov SM, Kalinin S, Chen Z, et al. Angiotensin I-converting enzyme Gln1069Arg mutation impairs trafficking to the cell surface resulting in selective denaturation of the C-domain. *PLoS One* 2010; **5**: e10438.

31. Kramers C, Danilov SM, Deinum J, et al. Point mutation in the stalk of angiotensin-converting enzyme causes a dramatic increase in serum angiotensin-converting enzyme but no cardiovascular disease. *Circulation* 2001; **104**: 1236–1240.

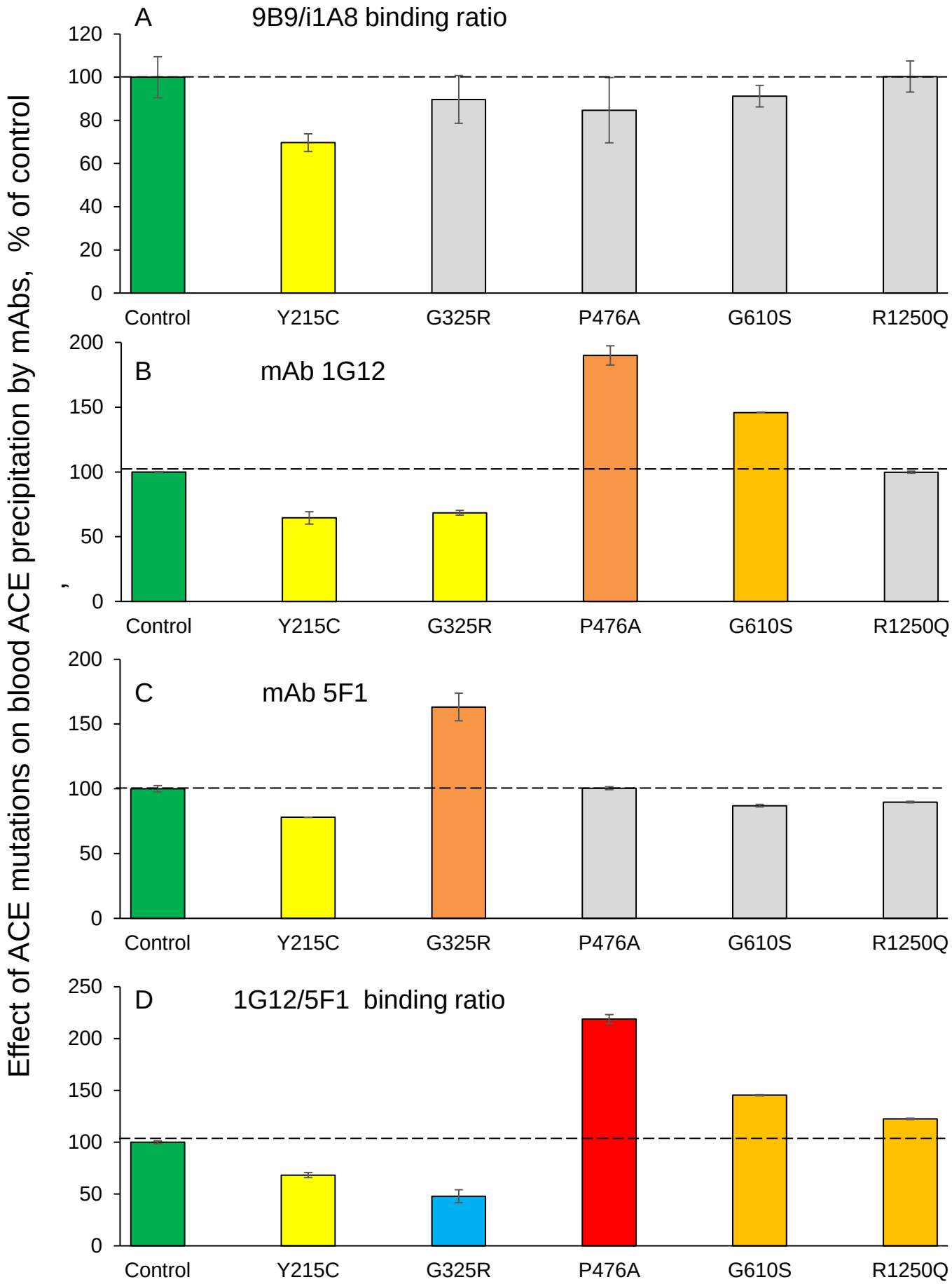
A
9B9/i1A8 binding ratio
120
100
80
60
40
20
0
Control
Y215C
G325R
P476A
G610S
R1250Q
B
mAb 1G12
200
150
100
50
0
C
mAb 5F1
D
1G12/5F1 binding ratio
250
Effect of ACE mutations on blood ACE precipitation by mAbs, % of control

Fig.S1.

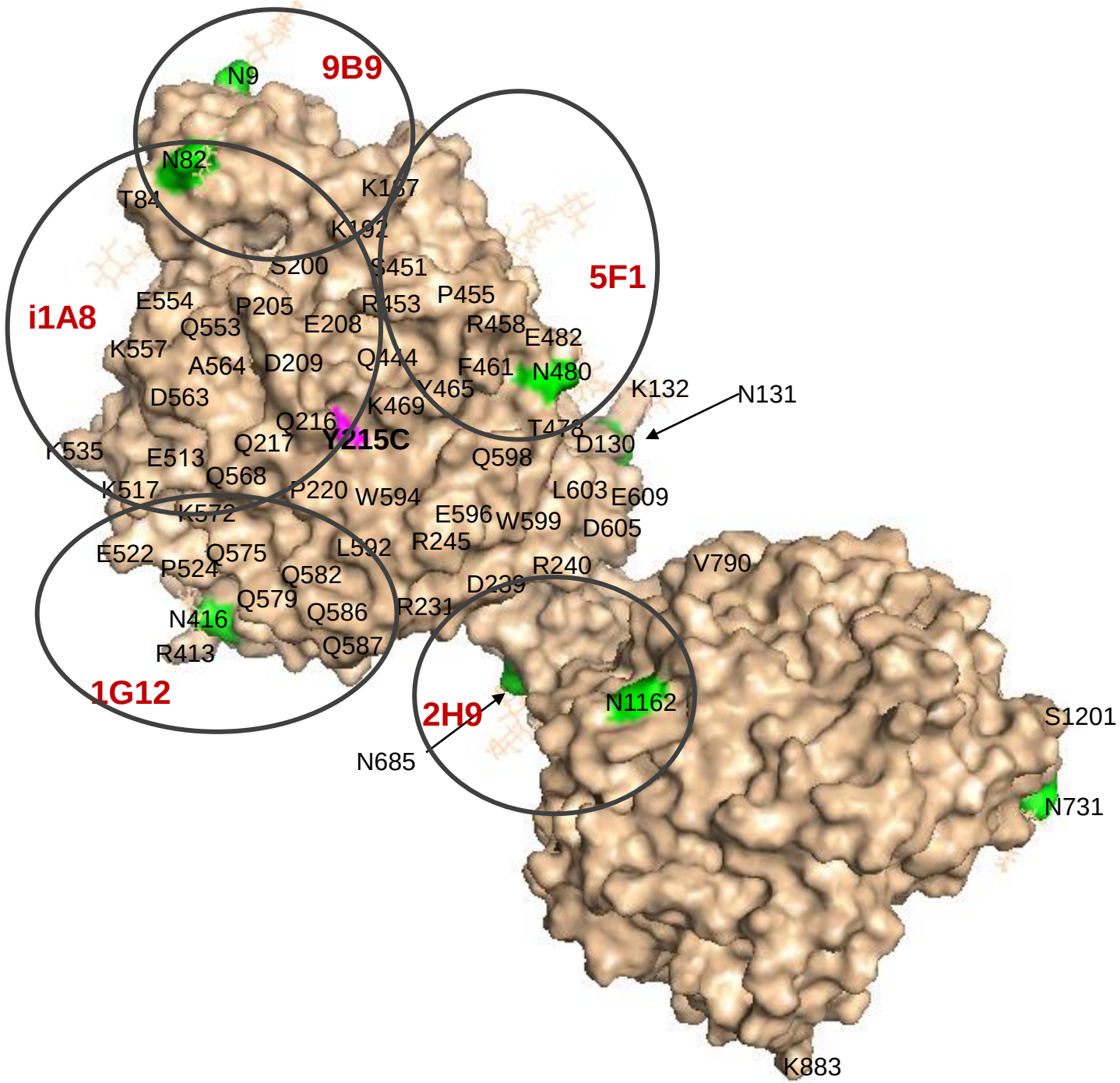
9B9
5F1
i1A8
1G12
2H9
N9
N82
T84
K137
K192
S200
S451
E554
P205
R453
P455
Q553
E208
R458
E482
K557
A564
D209
Q444
F461
N480
D563
Y465
K132
N131
K469
Q216
Y215C
T478
D130
K535
Q217
E513
Q598
Q568
K517
P220
W594
L603
E609
K572
E596
W599
D605
E522
Q575
L592
R245
P524
Q582
R240
V790
D239
Q579
Q586
R231
N416
Q587
R413
N1162
S1201
N685
N731
K883

Fig.S2.

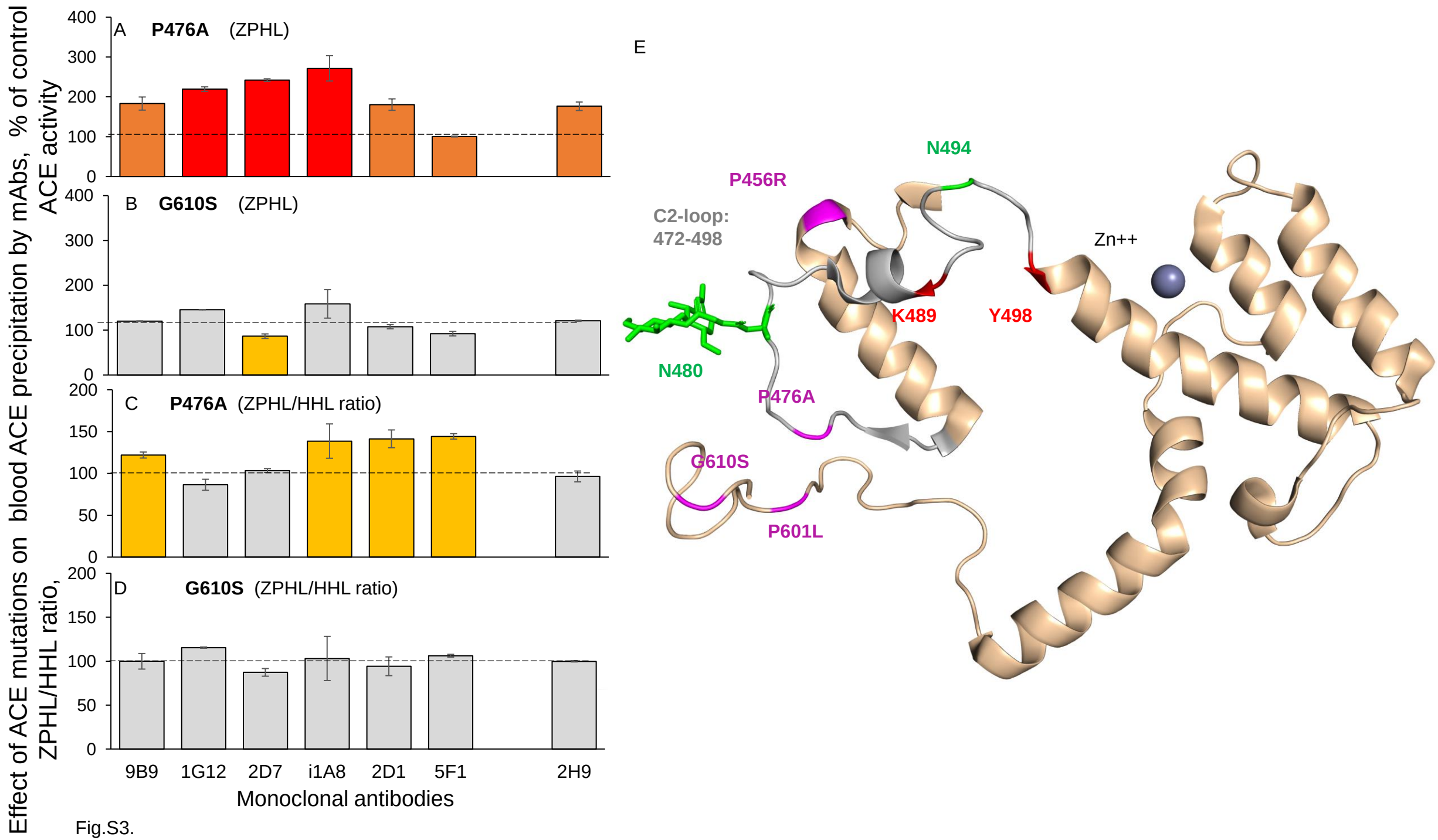
Effect of ACE mutations on blood ACE precipitation by mAbs, % of control ACE activity
ZPHL/HHL ratio,
A P476A (ZPHL)
B G610S (ZPHL)
C P476A (ZPHL/HHL ratio)
D G610S (ZPHL/HHL ratio)
400
300
200
100
0
150
50
9B9
1G12
2D7
i1A8
2D1
5F1
2H9
Monoclonal antibodies
E
N494
P456R
C2-loop:
472-498
Zn++
K489
Y498
N480
P476A
G610S
P601L

Fig.S3.

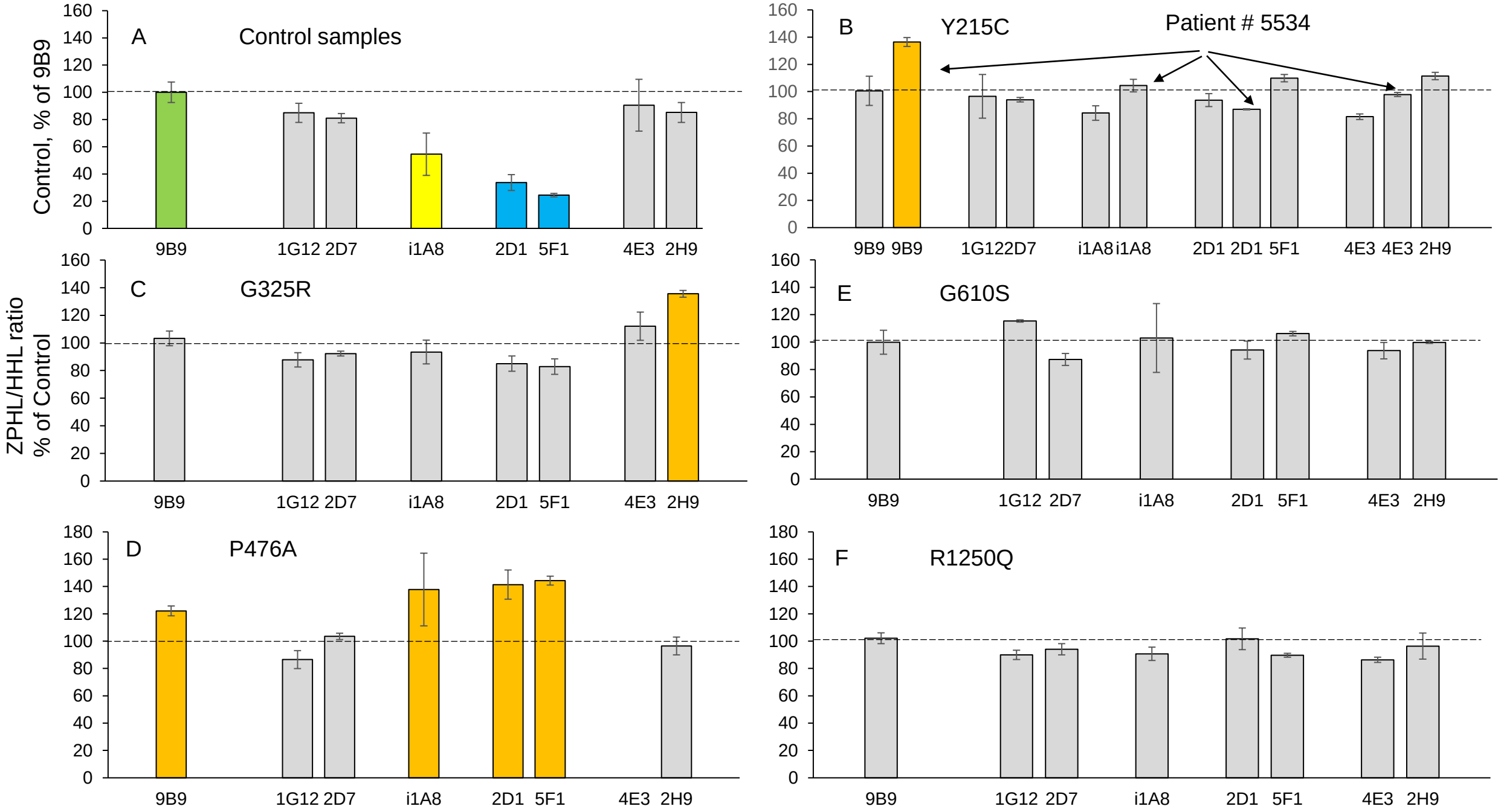
A
Control samples
Control, % of 9B9
B
Y215C
Patient # 5534
C
G325R
ZPHL/HHL ratio
% of Control
E
G610S
D
P476A
F
R1250Q
9B9
1G12
2D7
i1A8
2D1
5F1
4E3
2H9

Fig.S4.